Schultz, P. G., Taylor, J. S., & Dervan, P. B. (1982) *J. Am. Chem. Soc. 104*, 6861.
Sequin, U. (1974) *Helv. Chim. Acta 57*, 68.
Taylor, J. S., Schultz, P. G., & Dervan, P. B. (1984) *Tetrahedron 40*, 457.
Toulmé, J. J., Krish, H. M., Loreau, N., Thuong, N. T., & Hélene, C. (1986) *Proc. Natl. Acad. Sci. U.S.A. 83*, 1927.
Weil, G., & Calvin, M. (1963) *Biopolymers 1*, 401.
Zimmer, C., & Wähnert, U. (1986) *Prog. Biophys. Mol. Biol. 47*, 31.

# Comparative Circular Dichroism and Fluorescence Studies of Oligodeoxyribonucleotide and Oligodeoxyribonucleoside Methylphosphonate Pyrimidine Strands in Duplex and Triplex Formation†

Daniel E. Callahan, Tina L. Trapane, Paul S. Miller, Paul O. P. Ts'o, and Lou-Sing Kan*

*Department of Biochemistry, School of Hygiene and Public Health, The Johns Hopkins University, 615 North Wolfe Street, Baltimore, Maryland 21205*

*Received June 20, 1990; Revised Manuscript Received October 29, 1990*

ABSTRACT: An analogue of the homopyrimidine oligodeoxyribonucleotide $d(CT)_8$ has been synthesized. This analogue, $d(\underline{CT})_8$ contains nonionic methylphosphonate internucleoside linkages. The pH-dependent conformational transitions of $d(\underline{CT})_8$ have been studied and its ability to form duplexes and triplexes with the normal homopurine oligonucleotide $d(AG)_8$ has also been investigated as a function of pH. Circular dichroism spectroscopy and ethidium bromide fluorescence enhancement have been used to monitor pH-dependent conformational transitions driven by the protonation of cytosine residues, and the different behavior of $d(\underline{CT})_8$ and $d(CT)_8$ has been compared. It was possible to form self-associated complexes by using either $d(CT)_8$ or $d(\underline{CT})_8$, and both compounds combined with $d(AG)_8$ to form duplex or triplex DNA. At neutral pH, the CD spectrum of $d(AG)_8{\cdot}d(\underline{CT})_8$ duplex was quite different from the CD spectrum of $d(AG)_8{\cdot}d(CT)_8$ duplex, reflecting most likely a difference in conformation. The duplex to triplex transition characteristic of this DNA sequence occurred at a lower pH when $d(\underline{CT})_8$ was substituted for $d(CT)_8$; however, at pH 4.2, triplex containing $d(\underline{CT})_8$ was similar in conformation to triplex containing $d(CT)_8$. Several of these observations can be related to the alterations in electrostatic and steric interactions that occur when the negatively charged phosphodiester backbone of $d(CT)_8$ is replaced with a nonionic methylphosphonate backbone.

Oligodeoxyribonucleoside methylphosphonates are nucleic acid analogues containing nonionic methylphosphonate internucleoside linkages in place of the naturally occurring, negatively charged phosphodiester linkages (Miller & Ts'o, 1987). Methylphosphonates are nuclease-resistant and are taken up readily by mammalian cells in culture (Miller et al., 1981). One goal in the development of such compounds is the regulation of gene expression in living cells. Methylphosphonates can regulate gene expression at the level of mRNA translation by binding to complementary mRNA or precursor mRNA targets (Agris et al., 1986; Kean et al., 1988; Yu et al., 1989; Kulka et al., 1989). In such cases, duplex formation between the methylphosphonate and the mRNA target prevents the translation or processing of a particular mRNA transcript. Another goal in the development of these compounds is the regulation of gene expression at the transcriptional level by sequence-specific triplex formation with DNA. As has been recently described, the target in this case is a double-stranded, duplex DNA rather than single-stranded mRNA (Maher et al., 1989). The presence of a third strand in the major groove of a DNA duplex could hinder the binding of proteins or enzymes and thus prevent the production of a particular mRNA transcript.

Methylphosphonate-substituted oligodeoxyribonucleotides can bind to single-stranded DNA, and the resultant hybrid duplexes (containing one phosphodiester strand and one methylphosphonate strand) have altered stability relative to phosphodiester duplexes (Quartin & Wetmur, 1989). The changes in stability are dependent upon ionic strength and are due in part to the alteration of electrostatic interactions that occur when negatively charged phosphodiester linkages are replaced with nonionic methylphosphonate linkages. A steric factor is also partially responsible for the altered stability of these hybrid duplexes. During synthesis of these compounds, one of the two stereoisomers (either $R_p$ or $S_p$ configuration) is formed at each methylphosphonate linkage (Miller et al., 1979); thus, preparations of fully substituted methylphosphonate oligomers are a mixture of diastereomers, making it difficult to assess the contribution of the steric factor to duplex stability. The studies presented here empirically assess the effect of methylphosphonate substitution on the conformation of a hybrid duplex or triplex of deoxyoligonucleotides.

†This work was supported in part by DOE (Grant DE-FG02-88ER60636) and by NCI (Grant 5 PO1 CA42762-03). Preliminary results have been presented at the 34th annual meeting of the Biophysical Society, Baltimore, MD, February 1990.

*To whom correspondence should be addressed.

0006-2960/91/0430-1650$02.50/0 

Additionally, the impact of methylphosphonate substitution on the apparent $pK_a$ of triplex formation is examined.

Formation of triple-stranded polydeoxynucleotide helices has been well documented for the poly[d(A-G)·d(C-T)] to poly[d($C^+$-T)·d(A-G)·d(C-T)] transition at acidic pH (Morgan & Wells, 1968; Lee et al., 1979; Gray et al., 1987). Ethidium bromide (EB)[1] fluorescence enhancement is useful as a probe of DNA conformation (Morgan et al., 1979), and the use of EB fluorescence enhancement as an indicator of triplex formation has been demonstrated for poly[d(A-G)·d(C-T)] (Lee et al., 1979, 1984). In the formation of triple-stranded DNA, a third pyrimidine deoxypolynucleotide strand is known to bind in the major groove of the DNA duplex, parallel to the purine strand (Moser & Dervan, 1987). It has been demonstrated that the presence of the third strand in the major groove diminishes the fluorescence enhancement normally seen when EB intercalates into double-stranded DNA (Lee et al., 1979, 1984). Thus, for the sequence studied here, formation of deoxyoligonucleotide triplex may be monitored by observing the decrease in EB fluorescence as a function of pH. Additionally, the circular dichroism (CD) spectra of poly[d(A-G)·d(C-T)] and poly[d($C^+$-T)·d(A-G)·d(C-T)] have been reported (Lee et al., 1979; Gray et al., 1987), and the unique changes that occur in the CD spectrum are useful for monitoring the duplex to triplex conformational transition.

High-resolution NMR studies have indicated that oligonucleotides of this same sequence undergo a duplex to triplex transition similar to that seen in polymers (Rajagopal & Feigon, 1989a,b). The pyrimidine·purine·pyrimidine base triads that form in these triple-stranded helices are $C^+$·G·C and T·A·T. Acidic pH is required for the protonation of cytosine residues, and for this reason the biological significance of such triple-stranded helices is uncertain. However, it has been demonstrated in both polymers and oligomers that substitution of 5-methylcytosine for cytosine results in triple-helix formation at neutral pH (Lee et al., 1984; Povsic & Dervan, 1989; Maher et al., 1989). Thus, the possibility exists that triple-stranded helix formation may occur in vivo, and it has been proposed that these unusual DNA conformations may play a role in gene regulation (Lee et al., 1987; Wells et al., 1988; Maher et al., 1989).

In this report, we use fluorescence and CD spectroscopy to show that the 16-base-pair oligodeoxyribonucleotides $d(CT)_8$ and $d(AG)_8$ form triple-stranded helices at acidic pH in a manner similar to their corresponding polymers, i.e., poly[d(A-G)] and poly[d(C-T)]. More importantly, it is also demonstrated that an oligonucleotide analogue containing nonionic methylphosphonate internucleoside linkages, $d(\underline{CT})_8$, can also combine with $d(AG)_8$ to form triple-stranded DNA at acidic pH. The studies presented here indicate that at low pH the conformations of the normal triplex composed of three charged phosphodiester strands and the hybrid triplex containing two uncharged methylphosphonate pyrimidine strands are similar, despite electrostatic and steric differences between phosphodiester and methylphosphonate backbones. At neutral pH, however, CD spectra indicate that the conformation of the hybrid duplex differs from that of a homoduplex containing only phosphodiester backbones. In addition, the pH at which the transition to triplex occurs is seen to be lower. An explanation of these effects is presented.

## Materials and Methods

*Synthesis, Purification, and Characterization of Oligomers.* The hexadecadeoxyribonucleotides $d(CT)_8$ and $d(AG)_8$ were synthesized on either a Biosearch or an Applied Biosystems automated DNA synthesizer and were purified by ion-exchange HPLC and gel electrophoresis. Extinction coefficients at 254 nm in 0.01 M Tris and 0.002 M $MgCl_2$ buffer, pH 8.2, were determined by enzymatic digestion with snake venom phosphodiesterase I (Pharmacia, Piscataway, NJ) (Miller et al., 1980). The values $5.75 \times 10^3$ L·mol·res$^{-1}$·cm$^{-1}$ for $d(CT)_8$ and $9.06 \times 10^3$ L·mol·res$^{-1}$·cm$^{-1}$ for $d(AG)_8$ were obtained.

The hexadecadeoxyribonucleoside methylphosphonate, $d(\underline{CT})_8$, was synthesized as previously described (Miller et al., 1986). This oligonucleotide analogue contains one phosphodiester internuceotide bond at the 5′ end, and the remaining nonionic methylphosphonate internucleoside linkages were synthesized without any attempt to separate the stereoisomers formed at the chiral phosphates. Purification was achieved by DEAE-cellulose chromatography and reverse-phase HPLC. An extinction coefficient at 254 nm of $5.32 \times 10^3$ L·mol·res$^{-1}$·cm$^{-1}$ was obtained by complete cleavage of the methylphosphonate base linkages in 1 M piperidine solution for 4 h at 37 °C (Murakami et al., 1985).

*Fluorescence and CD Studies as a Function of pH.* Fluorescence and CD studies were performed on DNA solutions containing a total base residue concentration of $7.75 \times 10^{-5}$ M. An extinction coefficient of 6500 L·mol$^{-1}$·cm$^{-1}$ was used for *Escherichia coli* strain K12 DNA (General Biochemicals). Solutions were unbuffered and contained 0.1 M NaCl and $1 \times 10^{-5}$ M EDTA. The pH of the solutions was monitored by directly inserting a combination pH electrode designed for microsamples (Wilmad Glass, Buena, NJ) into 1-cm fluorescence sample cuvettes containing 1.0 or 1.5 mL of sample. The pH of the sample was adjusted by adding dilute HCl or NaOH in 1-μL increments. In the fluorescence studies this resulted in less than 2% dilution of the sample over the course of an experiment. In the CD studies the dilution was 2–4%. CD spectra were corrected for this dilution effect, but fluorescence readings were not.

*Ethidium Bromide Fluorescence Enhancement Studies.* The EB fluorescence enhancement studies were performed by adding a 10-μL aliquot of concentrated EB (Sigma, St. Louis, MO) solution directly into a 1-cm fluorescence sample cuvette containing 1.5 mL of DNA at a total base residue concentration of $7.75 \times 10^{-5}$ M. The final EB concentration was 0.5 μg/mL. Uncorrected fluorescence readings were taken manually at room temperature on an Aminco-Bowman spectrophotofluorometer with 4-mm slit widths. Emission was observed at 600 nm. Excitation spectra were taken between 285 and 565 nm and were similar to published DNA EB fluorescence enhancement spectra (LePecq & Paoletti, 1967). For pH-dependent studies, excitation was at 523 nm and emission was observed at 600 nm. A solution of *E. coli* DNA at a total base residue concentration of $7.75 \times 10^{-5}$ M was used as a fluorescence intensity standard. Spectra are reported by using arbitrary fluorescence units.

*CD Spectroscopy and Calculations.* CD spectra were obtained on an AVIV 60DS CD spectropolarimeter (AVIV Associates, Lakewood, NJ). The instrument was calibrated by using (1*S*)-(+)-10-camphorsulfonic acid (Aldrich, Milwaukee, WI). Spectra were obtained at 0.5- or 1.0-nm increments with a constant bandwidth of 0.8 nm. Temperature was maintained at 21.2 ± 0.1 °C by using a Neslab RTE-4DD

[1] Abbreviations: $d(AG)_8$, d-Ap(GpAp)$_7$G; $d(CT)_8$, d-Cp(TpCp)$_7$T; $d(\underline{CT})_8$, d-Cp(T*p*Cp)$_7$T, where *p* represents the 3′–5′ internucleoside methylphosphonate linkage in either the $R_p$ or $S_p$ configuration; EB, ethidium bromide; CD, circular dichroism; HPLC, high-performance liquid chromatography; DEAE, diethylaminoethyl; Tris, tris(hydroxymethyl)aminomethane; EDTA, ethylenediaminetetraacetic acid; UV, ultraviolet; $T_m$, melting temperature; res, residue.

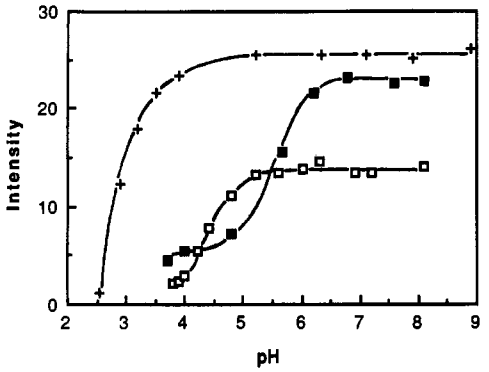


FIGURE 1: EB fluorescence assay of triplex formation as a function of pH: ■, 2:1 $d(CT)_8$:$d(AG)_8$; □, 2:1 $d(\underline{CT})_8$:$d(AG)_8$; and +, *E. coli* DNA. Excitation was at 523 nm, and emission was observed at 600 nm. All solutions are unbuffered in 0.1 M NaCl, $1 \times 10^{-5}$ M EDTA, and 0.5 μg/mL EB. Total base residue concentration is $7.75 \times 10^{-5}$ M.

refrigerated cooling bath (Neslab, Portsmouth, NH). Three scans at each pH value were obtained and averaged on a dedicated microcomputer. A baseline was subtracted and the data were smoothed on a IBM PS/2 Model 60 using software supplied by AVIV Associates. CD calculations were also performed with this software.

## Results

*Ethidium Bromide Fluorescence Enhancement Studies.* The fluorescence enhancements of *E. coli* DNA, 2:1 d-$(CT)_8$:$d(AG)_8$ and 2:1 $d(\underline{CT})_8$:$d(AG)_8$ solutions as a function of pH are plotted in Figure 1. The fluorescence enhancement of *E. coli* DNA was constant until a pH of approximately 4.5 and then it dropped to approximately zero by pH 2.5. The fluorescence enhancement of 2:1 $d(CT)_8$:$d(AG)_8$ was only slightly less than that of *E. coli* DNA between pH 8.2 and 7.0 but began to drop between pH values of 6.5 and 5.0, indicating formation of triple-stranded DNA in this region. At high pH, the fluorescence enhancement of 2:1 d-$(\underline{CT})_8$:$d(AG)_8$ is much less than that of *E. coli* DNA or 2:1 $d(CT)_8$:$d(AG)_8$. In addition, the transition of 2:1 d-$(\underline{CT})_8$:$d(AG)_8$ to triple-stranded helix has an apparent $pK_a$ of 4.5, while the apparent $pK_a$ of triplex formation appears to be 5.6 in the case of 2:1 $d(CT)_8$:$d(AG)_8$ (Figure 1).

*Circular Dichroism Studies.* The CD spectra of single-stranded $d(CT)_8$ and $d(\underline{CT})_8$ at 21.2 °C were seen to be dependent upon pH (Figure 2A). In both cases, the positive CD band was red-shifted from 275 to 282 nm as the pH was lowered from 6.8 to 4.2. While both $d(CT)_8$ and $d(\underline{CT})_8$ had similar CD spectra at pH 6.8, $d(\underline{CT})_8$ exhibited CD bands of greater intensity at pH 4.2 (Figure 2A). Both compounds exhibited a similar amount of red shift at low pH, and in both cases, the red shift occurred at approximately pH 5.5 (data not shown). As seen in Figure 2B, the CD spectrum of $d(AG)_8$ did not change greatly between pH 7.0 and 5.5.

The pH dependence of CD spectra was also monitored for 2:1 $d(CT)_8$:$d(AG)_8$ and 2:1 $d(\underline{CT})_8$:$d(AG)_8$. In the case of 2:1 $d(CT)_8$:$d(AG)_8$, a conformational transition was seen to occur between pH 6.8 and 5.2 (Figure 3A). The large negative band observed at 215 nm is believed to be indicative of a DNA triplex in the case of this particular sequence (Lee et al., 1979; Gray et al., 1987). A conformational transition was also observed for 2:1 $d(\underline{CT})_8$:$d(AG)_8$ as the pH was lowered (Figure 3B). At low pH, the CD spectra of 2:1 $d(CT)_8$:$d(AG)_8$ and 2:1 $d(\underline{CT})_8$:$d(AG)_8$ were quite similar, indicating that triple-stranded helix formed in both instances (Figure 3C). Figure 4 is a plot of $\Delta\epsilon$ at 215 nm versus pH for 2:1 d-$(CT)_8$:$d(AG)_8$ and 2:1 $d(\underline{CT})_8$:$d(AG)_8$ triplex formation. While the apparent $pK_a$ for 2:1 $d(CT)_8$:$d(AG)_8$ triplex formation was approximately 6.2, the apparent $pK_a$ for 2:1 d-$(\underline{CT})_8$:$d(AG)_8$ triplex formation was approximately 5.2.

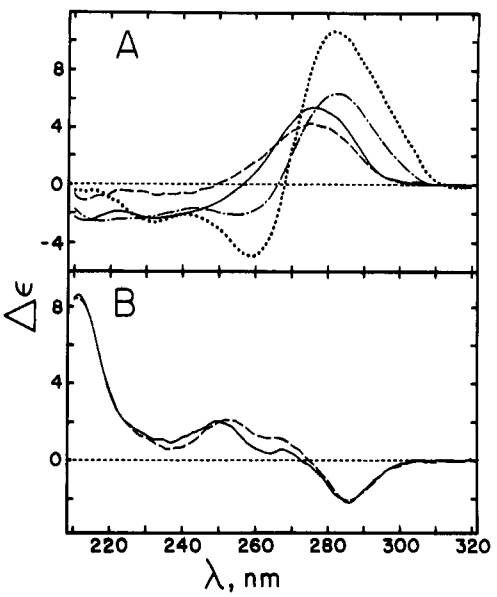


FIGURE 2: CD spectra at 21.2 °C of single-stranded $d(CT)_8$, $d(\underline{CT})_8$, and $d(AG)_8$ as a function of pH in 0.1 M NaCl and $1 \times 10^{-5}$ M EDTA. Total base residue concentration is $7.75 \times 10^{-5}$ M. (A) $d(CT)_8$ at pH 6.7 (—) and pH 4.2 (-·-); $d(\underline{CT})_8$ at pH 6.8 (---) and pH 4.2 (···). (B) $d(AG)_8$ at pH 7.0 (—) and pH 5.5 (---).

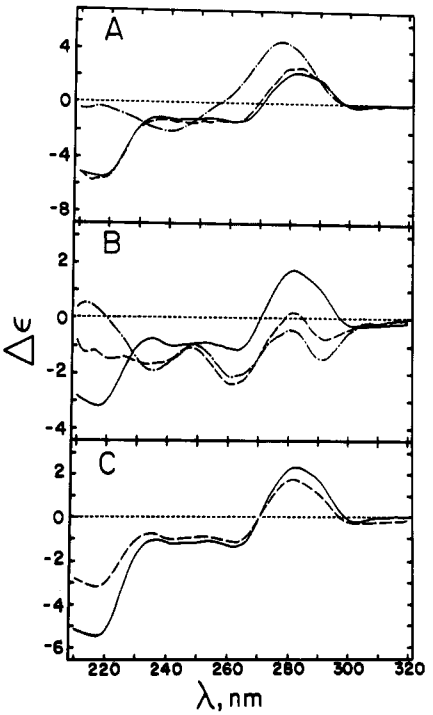


FIGURE 3: CD spectra at 21.2 °C for 2:1 $d(CT)_8$:$d(AG)_8$ and 2:1 $d(\underline{CT})_8$:$d(AG)_8$ at various pH values in 0.1 M NaCl and $1 \times 10^{-5}$ M EDTA. Total base residue concentration is $7.75 \times 10^{-5}$ M. (A) 2:1 $d(CT)_8$:$d(AG)_8$ at pH 6.8 (-·-), pH 5.2 (---) and pH 4.1 (—). (B) 2:1 $d(\underline{CT})_8$:$d(AG)_8$ at pH 6.8 (-·-), pH 5.2 (---) and pH 4.2 (—). (C) Comparison of 2:1 $d(CT)_8$:$d(AG)_8$ at pH 4.1 (—) and 2:1 $d(\underline{CT})_8$:$d(AG)_8$ at pH 4.2 (---).

In addition to the difference seen in the apparent $pK_a$ of triplex formation, a large difference was also observed in the CD spectra obtained at neutral pH when $d(\underline{CT})_8$ was substituted for $d(CT)_8$. At pH 6.8 the CD spectrum of 2:1 d-$(\underline{CT})_8$:$d(AG)_8$ was quite different from that observed for 2:1

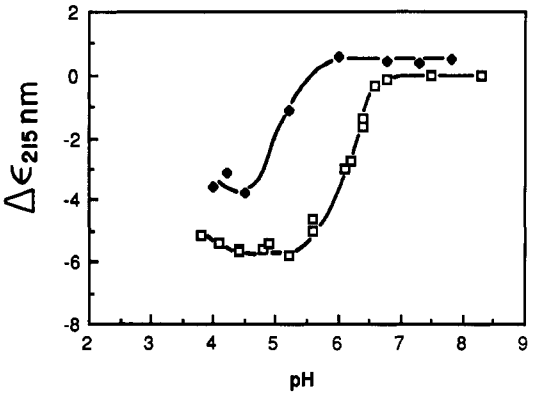


FIGURE 4: Triplex formation as a function of pH, estimated by using the negative CD band at 215 nm as an indication of triplex formation: □, 2:1 $d(CT)_8$:$d(AG)_8$; ◆, 2:1 $d(\underline{CT})_8$:$d(AG)_8$. Sample conditions are given in Figure 3.

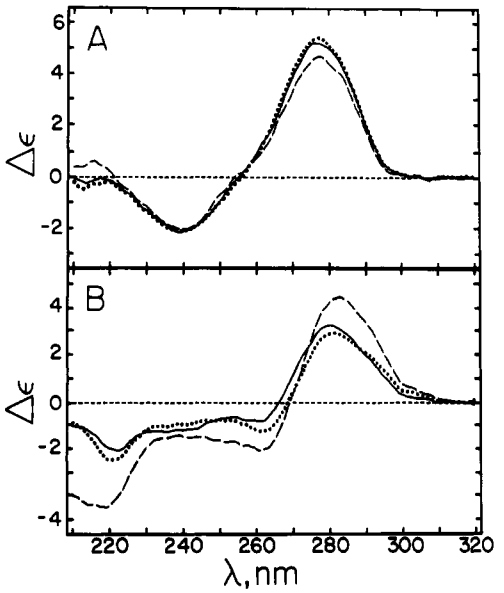


FIGURE 5: Comparison of calculated and observed CD spectra for 2:1 and 1:1 $d(CT)_8$:$d(AG)_8$. (A) 1:1 experimental spectrum at pH 7.0 (—); 2:1 experimental spectrum at pH 7.0 (---); spectrum calculated by taking the weighted average of spectra of single-stranded $d(CT)_8$ and duplex, both at pH 7.0 (···). (B) 1:1 experimental spectrum at pH 5.5 (—); 2:1 experimental spectrum at pH 5.5 (---); spectrum calculated by taking the weighted average of spectra of single-stranded $d(AG)_8$ and triplex, both at pH 5.5 (···).

$d(CT)_8$:$d(AG)_8$ (Figure 3A,B). The CD spectra at pH 7.0 of 1:1 $d(CT)_8$:$d(AG)_8$ (Figure 5A) and 1:1 $d(\underline{CT})_8$:$d(AG)_8$ (Figure 6) are similar to those seen for the 2:1 mixtures. As discussed below, any observed differences between 1:1 and 2:1 mixtures at neutral pH can be explained as being due to the presence of excess single-stranded $d(CT)_8$ or $d(\underline{CT})_8$.

*CD Calculations.* The observed differences between the CD spectra of 1:1 and 2:1 $d(CT)_8$:$d(AG)_8$ at pH 7.0 can be explained by weighting the observed duplex CD spectrum with a spectral contribution from free single-stranded $d(CT)_8$ (Figure 5A). Similar results were obtained for 2:1 $d(\underline{CT})_8$:$d(AG)_8$ at high pH (data not shown). This indicates that the third strand, $d(CT)_8$ or $d(\underline{CT})_8$, respectively, does not interact with the duplex at high pH. Similarly, when the pH of 1:1 $d(CT)_8$:$d(AG)_8$ is lowered to 5.5, the resulting CD spectrum is different from that observed for a 2:1 mixture at the same pH (Figure 5B). As shown by the calculated curve, this difference can be explained by taking into account a CD contribution from free, single-stranded $d(AG)_8$, which is present in excess after the duplex dismutates to form triple-

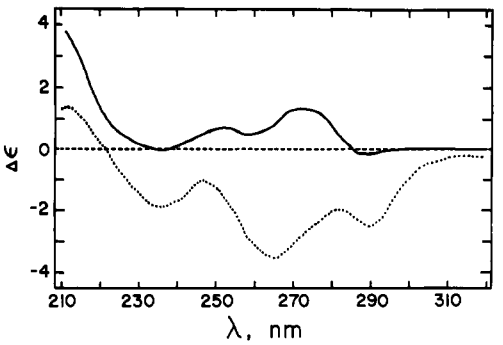


FIGURE 6: Comparison of calculated CD spectrum for noninteracting $d(AG)_8$ and $d(\underline{CT})_8$ single strands (—) and observed CD spectra for 1:1 $d(\underline{CT})_8$:$d(AG)_8$ (···). Calculated CD spectrum is the weighted average of single-stranded $d(\underline{CT})_8$ and single-stranded $d(AG)_8$ at pH 7.0.

stranded helix at low pH. These results indicate that the triplex and the free $d(AG)_8$ do not interact under these conditions. In addition, the CD spectrum of 1:1 $d(\underline{CT})_8$:$d(AG)_8$ is not simply the weighted average of free, single-stranded $d(\underline{CT})_8$ and single-stranded $d(AG)_8$ (Figure 6).

## Discussion

For the nucleic acid sequence studied here, our results indicate that both phosphodiester and methylphosphonate pyrimidine strands can form pyrimidine·pyrimidine self-associated complexes, pyrimidine·purine duplexes, and pyrimidine·purine·pyrimidine triplex DNA. However, the substitution of $d(\underline{CT})_8$ for $d(CT)_8$ does appear to alter the conformation of self-associated complexes, duplexes, and triplexes to some extent. In addition, the apparent $pK_a$ of the duplex to triplex transition is decreased when $d(\underline{CT})_8$ is substituted for $d(CT)_8$. Several important consequences of methylphosphonate substitution are discernible in these alterations of conformation or pH-dependent conformational transitions.

For single-stranded $d(CT)_8$ and $d(\underline{CT})_8$, the pH-dependent CD spectra indicate the formation of an ordered complex at low pH (Figure 2A), possibly a self-associated complex similar to that postulated for poly[d(C-T)] (Gray et al., 1987). As judged by the changes in the CD spectra, single-stranded $d(\underline{CT})_8$ appears to undergo a much more significant conformational transition when the pH is lowered. At 21 °C, the low-pH CD spectrum of $d(CT)_8$ is diminished in magnitude, possibly indicating that this self-associated complex has less structure than that formed by $d(\underline{CT})_8$. Such an interpretation of the CD results is supported by the fact that both self-associated pyrimidine strands exhibit cooperative UV melting transitions at low pH, with the $T_m$ for the methylphosphonate complex (40 °C) being substantially higher than that for the phosphodiester complex (15 °C) (data not shown). It has been postulated that, in the poly d(C-T) self-associated complex, the thymine bases must loop out into the solution in order for the $C^+$·C base pairs to form. Self-associated complexes of $d(\underline{CT})_8$ may be more stable than those formed by $d(CT)_8$ because repulsions due to the negatively charged phosphate groups of looped-out thymine bases have been eliminated. Such repulsions have been postulated to have an effect on the stability of self-associated complexes formed by poly d(C-T) (Gray et al., 1987).

At neutral pH, both CD spectroscopy and, to a lesser extent, EB fluorescence enhancement indicate that duplexes of $d(\underline{CT})_8$:$d(AG)_8$ form and are different in conformation than duplexes of $d(CT)_8$:$d(AG)_8$. The CD spectrum of 1:1 $d(\underline{CT})_8$:$d(AG)_8$ (Figure 6) differs greatly from that of 1:1 d-

$(CT)_8$:$d(AG)_8$ (Figure 5A). While the CD spectrum of the latter is characteristic of B-form DNA, the CD spectrum of 1:1 $d(\underline{CT})_8$:$d(AG)_8$ is composed of three negative bands between 230 and 290 nm and cannot be assigned to any canonical form of DNA. As demonstrated in Figure 6, CD calculations indicate that the single strands $d(\underline{CT})_8$ and $d(AG)_8$ do associate and form a hybrid duplex, because the observed CD spectrum cannot be explained as the sum of free, noninteracting single strands. Additional evidence for the formation of a hybrid duplex, to be published elsewhere, includes UV mixing and melting curves, as well as NMR studies which confirm that a 1:1 complex is formed that possesses a typical two-state helix-to-coil transition and hydrogen-bonded imido resonances assigned to Watson–Crick G·C and A·T base pairs. A difference in duplex conformation may be one reason why the 2:1 $d(\underline{CT})_8$:$d(AG)_8$ mixture produces less EB fluorescence enhancement than 2:1 $d(CT)_8$:$d(AG)_8$ at high pH (Figure 1). It should be noted, however, that although the magnitude of the enhancement is decreased, the amount of enhancement observed does indicate that a hybrid duplex has formed.

A combination of electrostatic and steric effects due to the presence of one nonionic methylphosphonate backbone containing a mixture of stereoisomers may produce the altered duplex conformation observed here. Given the large effect seen on duplex conformation, it is surprising that a triplex containing two methylphosphonate pyrimidine strands is very similar in conformation to normal triplex DNA (Figure 3C). However, the effects of methylphosphonate substitution are evident when the pH dependence of the duplex to triplex transition is examined.

In studies of the duplex to triplex transition, the EB fluorescence enhancement results are consistent with the CD results because both techniques indicate that 2:1 $d(CT)_8$:$d(AG)_8$ triplex forms at a higher pH than 2:1 $d(\underline{CT})_8$:$d(AG)_8$ triplex. The fluorescence assay indicates that while both triplexes have formed by pH 4.0, the apparent $pK_a$ of triplex formation is 5.6 for the 2:1 $d(CT)_8$:$d(AG)_8$ triplex and 4.5 for the 2:1 $d(\underline{CT})_8$:$d(AG)_8$ triplex (Figure 1). CD spectra taken over this pH range support such an interpretation of the fluorescence data. Figure 3A shows the CD spectrum characteristic of triplex DNA at pH 5.2 for 2:1 $d(CT)_8$:$d(AG)_8$, but a similar CD spectrum was not observed for 2:1 $d(\underline{CT})_8$:$d(AG)_8$ until pH 4.1 (Figure 3B). At pH 4.1, both compounds appear to have formed triple-stranded DNA with approximately the same overall conformation (Figure 3C). It should be noted that the distinctive triplex CD spectrum observed here has also been observed for NMR samples of 2:1 $d(CT)_8$:$d(AG)_8$ at 1000-fold greater concentrations, under conditions where the presence of triplex has been unambiguously determined by NMR spectroscopy (unpublished data).

For this DNA sequence, $\Delta\epsilon$ at 215 nm may be used to monitor triplex formation (Lee et al., 1979; Gray et al., 1987). As seen in Figure 4, apparent $pK_a$s of 6.2 and 5.2 are observed for 2:1 $d(CT)_8$:$d(AG)_8$ and 2:1 $d(\underline{CT})_8$:$d(AG)_8$ triplex formation, respectively. EB fluorescence assays (Figure 1) seem to consistently indicate lower apparent $pK_a$s than the titrations monitored by CD spectroscopy. It is known that the intercalation of EB stabilizes duplex DNA and causes an increase in the melting temperature (LePecq & Paoletti, 1967; Patel & Canuel, 1976). This may explain the discrepancies observed between the EB fluorescence enhancement $pK_a$s and those obtained by CD spectroscopy in the absence of EB. If the duplex conformation is stabilized by the presence of intercalated EB, it is possible that lower pH values may be required to drive the duplex to triplex conformational transition.

Triplex formation involves the protonation of cytosine and the formation of $C^+$·G·C base triads. This protonation provides two features favorable to the stability of the triplex, a positive charge for interactions with the negatively charged phosphate groups in the backbone and a proton for the formation of a hydrogen bond. Such factors have been seen to play a role in the formation of double-stranded protonated helical structures of poly[d(C)] at neutral pH (Akinrimisi et al., 1963; Inman, 1964; Hartman & Rich, 1965; Gray et al., 1987). These complexes contain $C^+$·C base pairs. The large shift in apparent $pK_a$ values from 4.5 for the cytosine monomer to above 7.0 for the poly[d(C)] (Gray et al., 1987) is attributed to the stabilization of the protonated form by hydrogen-bonding and electrostatic interactions with the phosphodiester backbone (Hartman & Rich, 1965). As expected, this stabilization is strongly dependent upon ionic strength. Higher ionic strengths destabilize these complexes; thus, $T_m$ is seen to increase with decreasing ionic strength (Akinrimisi et al., 1963; Inman, 1964; Hartman & Rich, 1965).

The loss of favorable interactions between the negatively charged phosphodiester backbones and positively charged protonated cytosines may be one factor responsible for the low apparent $pK_a$ of 2:1 $d(\underline{CT})_8$:$d(AG)_8$ triplex formation. Positive charges that develop on $C^+$·G·C base triads can interact favorably with three negatively charged phosphodiester backbones in the 2:1 $d(CT)_8$:$d(AG)_8$ triplex. As determined by EB fluorescence assays, in this case the apparent $pK_a$ of triplex formation is 5.6 (Figure 1). When two of the three negatively charged backbones are neutralized, as is the case for the 2:1 $d(\underline{CT})_8$:$d(AG)_8$ triplex, then the apparent $pK_a$ becomes 4.5 (Figure 1), close to that of the cytosine monomer (Gray et al., 1987).

It should be noted, then, that the 2:1 $d(\underline{CT})_8$:$d(AG)_8$ triplex is not an ideal model system for the study of methylphosphonate third strands interacting with an all-phosphodiester Watson–Crick DNA duplex, which is the situation expected in vivo. However, results presented here indicate that it may be possible to add single-stranded $d(\underline{CT})_8$ to a 1:1 $d(CT)_8$:$d(AG)_8$ duplex and study the binding of $d(\underline{CT})_8$ as the third strand. As seen in Figure 3, panels A and B, at pH 6.8 the CD spectra of 2:1 $d(CT)_8$:$d(AG)_8$ and 2:1 $d(\underline{CT})_8$:$d(AG)_8$ are almost inverted with respect to each other. The different CD spectra of the 1:1 $d(CT)_8$:$d(AG)_8$ duplex (Figure 5A) and the 1:1 $d(\underline{CT})_8$:$d(AG)_8$ duplex (Figure 6) are responsible for this inversion. Thus, if $d(\underline{CT})_8$ is added to a 1:1 $d(CT)_8$:$d(AG)_8$ duplex and strand exchange occurs, this will be immediately evident in the observed CD spectrum. Preliminary experiments have been performed (unpublished data), and CD spectroscopy indicates that no strand exchange occurs in such instances. Preliminary EB fluorescence assays have also been performed, and the apparent $pK_a$ of 1:1:1 $d(CT)_8$:$d(AG)_8$:$d(\underline{CT})_8$ triplex formation is approximately 5.4, intermediate in value between the apparent $pK_a$s of 4.5 for 2:1 $d(\underline{CT})_8$:$d(AG)_8$ and 5.6 for 2:1 $d(CT)_8$:$d(AG)_8$. CD spectra of 1:1:1 $d(CT)_8$:$d(AG)_8$:$d(\underline{CT})_8$ at pH 5.5 also indicate the formation of triplex. This preliminary data lends support to the argument that triplexes form at higher pH when they are stabilized by favorable interactions between protonated cytosines and negatively charged phosphodiester backbones.

ACKNOWLEDGMENTS

We are grateful to Kathy Meade for synthesizing and purifying the methylphosphonate oligomers and to Scott Morrow of the Department of Biochemistry DNA Synthesis Facility for preparing the phosphodiester oligomers used in these

studies. Also, we would like to thank Dr. David Shortle, Department of Biological Chemistry, The Johns Hopkins School of Medicine, for providing the CD spectrometer.

REFERENCES

Agris, C. H., Blake, K. R., Miller, P. S., Reddy, M. P. & Ts'o, P. O. P. (1986) *Biochemistry 25*, 6268-6275.
Akinrimisi, E. O., Sander, C., & Ts'o, P. O. P. (1963) *Biochemistry 2*, 340-344.
Gray, D, M., Ratliff, R. L., Antao, V. P., & Gray, C. W. (1987) in *Structure and Expression: DNA and Its Drug Complexes* (Sarma, R. H., & Sarma, M. H., Eds.) Vol. II, pp 147-166, Adenine Press, New York.
Hartman, K. A., Jr., & Rich, A. (1965) *J. Am. Chem. Soc. 87*, 2033-2039.
Inman, R. B. (1964) *J. Mol. Biol. 9*, 624-637.
Kean, J. M., Murakami, A., Blake, K. R., Cushman, C. D., & Miller, P. S. (1988) *Biochemistry 27*, 9113-9121.
Kulka, M., Smith, C., Aurelian, L. Fishelevich, R., Meade, K., Miller, P. S., & Ts'o, P. O. P. (1989) *Proc. Natl. Acad. Sci. U.S.A. 86*, 6868-6872.
Lee, J. S., Johnson, D. A., & Morgan, A. R. (1979) *Nucleic Acids Res. 9*, 3073-3091.
Lee, J. S., Woodsworth, M. L., Latimer, L. J. P., & Morgan, A. R. (1984) *Nucleic Acids Res. 12*, 6603-6614.
LePecq, J.-B., & Paoletti, C. (1967) *J. Mol. Biol. 27*, 87-106.
Maher, L. J., Wold, B., & Dervan, P. B. (1989) *Science 245*, 725-730.
Miller, P. S., & Ts'o, P. O. P. (1987) *Anti-Cancer Drug Des. 2*, 117-128.
Miller, P. S., Yano, J., Yano, E., Carroll, C., Jayaraman, K., & Ts'o, P. O. P. (1979) *Biochemistry 18*, 5134-5143.
Miller, P. S., Cheng, D. M., Dreon, N., Jayaraman, K., Kan, L.-S., Leutzinger, E. E., Pulford, S. M., & Ts'o, P. O. P. (1980) *Biochemistry 19*, 4688-4698.
Miller, P. S., McParland, K. B., Jayaraman, K., & Ts'o, P. O. P. (1981) *Biochemistry 20*, 1874-1880.
Miller, P. S., Reddy, M. P., Murakami, A., Blake, K. R., Agris, C. H., & Lin, S.-B. (1986) *Biochemistry 25*, 5092-5097.
Morgan, A. R., & Wells, R. D. (1968) *J. Mol. Biol. 37*, 63-80.
Morgan, A. R., Lee, J. S., Pulleybank, D. E., Murray, N. L., & Evans, D. H. (1979) *Nucleic Acids Res. 7*, 547-569.
Moser, H. E., & Dervan, P. B. (1987) *Science 238*, 645-650.
Murakami, A., Blake, K. R., & Miller, P. S. (1985) *Biochemistry 24*, 4041-4046.
Patel, D. J., & Canuel, L. L. (1976) *Proc. Natl. Acad. Sci. U.S.A. 73*, 3343-3347.
Povsic, T. J., & Dervan, P. B. (1989) *J. Am. Chem. Soc. 111*, 3059-3061.
Quartin, R. S., & Wetmur, J. G. (1989) *Biochemistry 28*, 1040-1047.
Rajagopal, P., & Feigon, J. (1989a) *Nature 339*, 637-640.
Rajagopal, P., & Feigon, J. (1989b) *Biochemistry 28*, 7859-7870.
Wells, R. D., Collier, D. A., Hanvey, J. C., Shimizu, M., & Wohlrab, F. (1988) *FASEB J. 2*, 2939-2949.
Yu, Z., Chen, D., Black, R. J., Blake, K., Ts'o, P. O. P., Miller, P., & Chang, E. H. (1989) *J. Exp. Pathol. 4*, 97-107.

# Recognition of *Escherichia coli* Valine Transfer RNA by Its Cognate Synthetase: A Fluorine-19 NMR Study†

Wen-Chy Chu and Jack Horowitz*
*Department of Biochemistry and Biophysics, Iowa State University, Ames, Iowa 50011*
*Received June 28, 1990; Revised Manuscript Received November 6, 1990*

ABSTRACT: Interactions of 5-fluorouracil-substituted *Escherichia coli* $tRNA^{Val}$ with its cognate synthetase have been investigated by fluorine-19 nuclear magnetic resonance. Valyl-tRNA synthetase (VRS) (EC 6.1.1.9), purified to homogeneity from an overproducing strain of *E. coli*, differs somewhat from VRS previously isolated from *E. coli* K12. Its amino acid composition and N-terminal sequence agree well with results derived from the sequence of the VRS gene [Heck, J. D., & Hatfield, G. W. (1988) *J. Biol. Chem. 263*, 868-877]. Apparent $K_M$ and $V_{max}$ values of the purified VRS are the same for both normal and 5-fluorouracil (FUra)-substituted $tRNA^{Val}$. Binding of VRS to (FUra)$tRNA^{Val}$ induces structural perturbations that are reflected in selective changes in the $^{19}F$ NMR spectrum of the tRNA. Addition of increasing amounts of VRS results in a gradual loss of intensity at resonances corresponding to FU34, FU7, and FU67, with FU34, at the wobble position of the anticodon, being affected most. At higher VRS/tRNA ratios, a broadening and shifting of FU12 and of FU4 and/or FU8 occur. These results indicate that VRS interacts with $tRNA^{Val}$ along the entire inside of the L-shape molecule, from the acceptor stem to the anticodon. Valyl-tRNA synthetase also causes a splitting of resonances FU55 and FU64 in the T-loop and stem of $tRNA^{Val}$, suggesting conformational changes in this part of the molecule. No $^{19}F$ NMR evidence was found for formation of the Michael adduct between VRS and FU8 of 5-fluorouracil-substituted $tRNA^{Val}$ that has been proposed as a common intermediate in the aminoacylation reaction.

Aminoacyl-tRNA synthetases catalyze the first step in protein biosynthesis, i.e., attachment of a specific amino acid to the 3′ end of its cognate tRNA. Because the fidelity of translation depends in large part on the specificity of this reaction, numerous experimental approaches have been employed to investigate the interaction between tRNA and aminoacyl-tRNA synthetases, including aminoacylation studies of chemically modified, mutant, or dissected tRNAs; protection

† Journal Paper No. J-14083 of the Iowa Agriculture and Home Economics Experiment Station, Ames, IA. Project No. 2566. This investigation was supported by NSF Grant DMB 87-04978.
* Address correspondence to this author.

0006-2960/91/0430-1655$02.50/0 